JOURNAL OF MULTIFUNCTIONAL MATERIALS & PHOTOSCIENCE
10(2), December 2019, pp. 223-235

Fabrication of Aluminum Doped Zinc Oxide (AZO) Transparent Conductive Oxide Thin Films by Spray Pyrolysis Technique

A. Jacquiline Regina Mary[1], S.Arumugam[2]

[1]*Department of Physics, Jayaraj Annapackiam College for Women (Autonomous), Periyakulam, Theni Dist, Tamilnadu*
[2]*Solar Energy Division, Department of Physics, The Gandhigram Rural Institute-Deemed University, Gandhigram, Dindigul Dist, Tamilnadu*

Abstract: Aluminum doped Zinc oxide (AZO) thin films with different Al content were deposited by spray pyrolysis and its structural, electrical and optical properties were studied. XRD pattern illustrate the films grow in the Wurtzite phase. Calculated texture coefficient [TC]hkl values showed the preferential growth along (100) plane. The FTIR spectrum for the AZO sample revealed the vibrational property through Zn-O stretching mode at 458cm-1 .The absorption edges are found to be blue shifted and the energy band gap values were estimated by Tauc relation increases from 3.21eV to 3.30eV. The widening of band gap is due to Burstein-Moss effect. The Optical parameters such as index of refraction (n) and extinction coefficient k (?) are observed to be consistent in the visible area, and tend to diminish with the addition of Al content. Doping also improves the conductivity by two orders of magnitude. A minimum resistivity of 0.45? cm and a transmittance of 72% at 550nm was found for AZO film with doping ratio of 5%. The obtained results show that AZO film with 5% doping is appropriate as a transparent electrode in solar cell.

Keywords: Texture Coefficient; Refractive Index; Band gap; Electrical conductivity.

Introduction

Zinc oxide based transparent conducting oxide (TCO) films are being studied extensively because of its numerous technical applications. They have good optoelectronic properties which are much needed for the use as transparent electrodes in flat panel displays such as plasma display panels and electronic paper displays. Thin films of Zinc oxide are suitable candidates as antireflection coating in solar cells [1], heat mirrors and multi layer photo thermal conversion systems [2], gas sensors and spintronics [3], transparent thin film transistors, photo detectors, light emitting diodes and laser diodes that operate in the UV and blue region of the spectrum [4], catalyzers [5] etc. In addition ZnO thin film posse's high electro-chemical stability and absence of toxicity. ZnO is a n-type semiconductor with large band gap 3.37 eV and binding energy of 60 mev, high transparency and low resistivity in the visible region and posses high light trapping properties [6-8].Compared to indium tin oxide(ITO) , ZnO is abundance in nature and its non-toxicity, allows it to be a attractive TCO material.

2.1. Material synthesis

2.2. *Experimental setup*

The spray unit used was a indigenous set up comprising a burette, a glass nozzle and a temperature controller made from University Scientific Instrumentation Centre (USIC) meant for spraying good film. A PID temperature controller was used to heat the glass substrate upto 400±5ÚC. Compressed air was used as a carrier gas and the solution flow rate was kept at 4ml/ min. After coating, the films were allowed to cool to room temperature. The films were annealed at 500ÚC after deposition.

2.3. *Characterization technique*

The structural analysis was made by pan analytical XPERT-PRO X-ray diffractometer system with a scan angle from 20Ú to 80 Ú and the anode material as copper. The surface morphology was seen by TESCAN VEGA3 Scanning Electron microscope. The optical studies were carried out by UV-Vis spectrophotometer (Shimadzu, model UV-1800, Japan) in the wavelength range 190-1100nm. FTIR Spectra are recorded by Perkin Elmer BX II spectrometer between the wave number region 4000cm^{-1} to 400cm^{-1}. The Keithley source meter model 4600 was used to record the I-V characteristics of the samples. Hall measurement and sheet resistance of the AZO films are measured by van der Pauw method.

3. Results and discussion

3.1. *Structural analysis*

3.1.1 XRD pattern

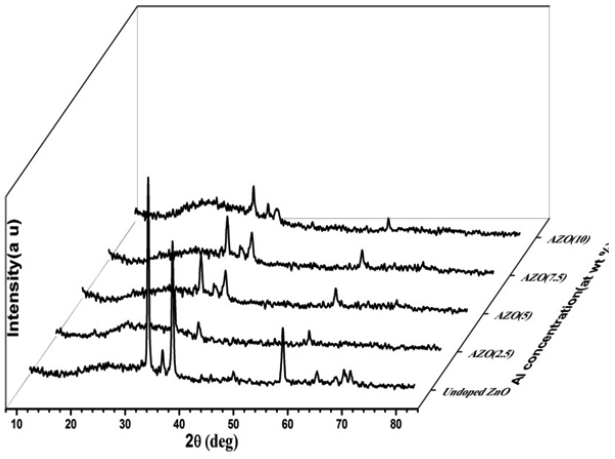

Figure 1: XRD pattern of undoped and Al doped ZnO thin films.

The XRD Spectra of pure ZnO an AZO films, for different doping percentages are shown in Figure1. The observed XRD pattern depicts the polycrystalline nature with hexagonal Wurtzite structure. The diffraction peaks (Miller indices) are found to match with the JCPDS card no: 36-1451.The prominent peaks are along (100), (002) ,(101) and (110) planes corresponding to the 2è values 31.81Ú, 34.41Ú, 36.36Ú and 56.53Úrespectively. There are small peaks noted along (102), (110), (112) diffraction planes for both pure ZnO and doped ZnO (AZO). As the Al doping concentration increases the intensity of the prominent as well as weaker diffraction peaks decrease indicating the degradation of crystalline nature of the films after doping . But there is no change in the preferred growth plane and the same trend is observed by F.Paraguay et.al in their research [23-25].

When the Al concentration is raised, the intensity of the (100) plane, which is dominant in the undoped and AZO 2.5 film continues to decrease, and the (002) peak start to appear for the doped AZO (5) and AZO (7.5) thin films. This implies that as the Al concentration increases, the growth of the films tends to align parallel to the c-axis. However, for all the as deposited and doped films the (100) plane is the prominent growth plane. For AZO(10) film the intensity of all the peaks become smaller and the films is amorphous ,indicating that increase in aluminum concentration leads to random orientation. K.L Chopra et.al in their study discussed that the ZnO crystals with lower surface energy prefer to grow along (002) diffraction plane [27]. Hence (100) orientation may be attributed to a little higher surface energy of the films grown perpendicular to the glass substrate. The preferential growth of the films can also be theoretically estimated from texture coefficient values, calculated from the XRD data. The texture co-efficient $[TC]_{hkl}$ symbolizes the texture of a diffraction plane and whenever this value deviates from unity that indicates the preferred growth. The texture co-efficient $[TC]_{\mathbf{hkl}}$ is expressed by [4].

$$TC_{(hkl)} = \frac{\dfrac{I_{(hkl)}}{I_{0(hkl)}}}{\dfrac{1}{N}\left[\sum \dfrac{I_{(hkl)}}{I_{0(hkl)}}\right]} \tag{1}$$

Where $I_{(hkl)}$ represents the measured value of intensity for a (hkl) plane and $I_{0(hkl)}$ is the standard intensity of the peak taken from JCPDS card data.The lattice parameters a (the second nearest neighbor distance) and c (the length of bond parallel to c-axis) are calculated from the d-spacing and the miller indices h, k and l through the expression [28] as,

$$\frac{1}{d^2} = \frac{4}{3}\,\frac{(\square^2+\square k+l^2)}{a^2} + \frac{l^2}{c^2} \tag{2}$$

The grain size is calculated through the Debye-Scherrer formula [29].

$$D = \frac{0.94\lambda}{\beta Cos\theta} \quad (3)$$

Where â is the width measured at half maximum intensity (FWHM) of the diffraction peak. ë is the wavelength of the Cu Ká ,X-ray radiation and its value is 1.5406$\dot{A}$ and è is the Bragg's angle. The estimated lattice constants and the grain size are listed in Table 1.

Table 1: **Variation of grain size and lattice constants with Al dopant concentration.**

Al Concentration(at .wt %)	Grain size(nm)	$[TC]_{hkl}(100)$	Lattice constants	
			a	c
0%	28.88	1.38	3.19	5.21
2.5%	21.87	2.14	3.20	5.19
5%	55.61	1.92	3.24	5.18
7.5%	16.12	1.39	3.21	5.18
10%	27.94	1.64	3.16	5.23

The crystalline particle size decreases for Al doped films compared to the undoped ZnO, except AZO (5). This is attributed to the disorder developed in the lattice for higher Al concentration, owing to the difference in the ionic radii of Zn^{2+} (r_{Zn}^{2+} = 0.074nm) and Al^{3+} (r_{Al}^{3+}=0.057nm) [5] .

3.1.2 FTIR studies

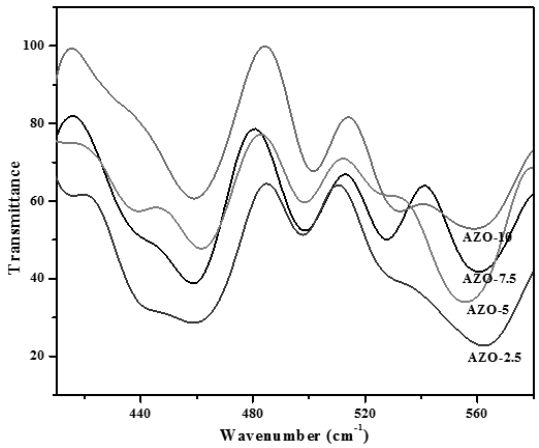

Figure 2: The Fourier Transform Infra Red transmission spectra of AZO thin films deposited at different Al concentrations

FTIR spectroscopy supplies the information about the occurence of elements in the sample. Figure 2 shows the FTIR spectrum of AZO thin films recorded from 4000 to 400 cm^{-1}. The Fourier transform Infrared spectra recorded for AZO sample revealed the vibrational property through Zn-O stretching mode at 458cm^{-1} which is characteristic vibration of ZnO. Inclusion of Al in the ZnO lattice is confirmed by the emergence of common band exists in all cases such as 568 cm^{-1}, 528 cm^{-1} and 498cm^{-1} which are

identified to be the characteristic bond of Al_2O_3 [11]. There is a shift observed in the IR transmittance spectrum of A ZO, which may be ascribed to the crystal perturbation introduced by the dopant atoms into the lattice sites.

3.1.3. Morphological studies

The surface morphological studies were carried out by scanning electron microscope (SEM) which shows the existence of nanostructure for the doped and as deposited thin films. (Figure 3)

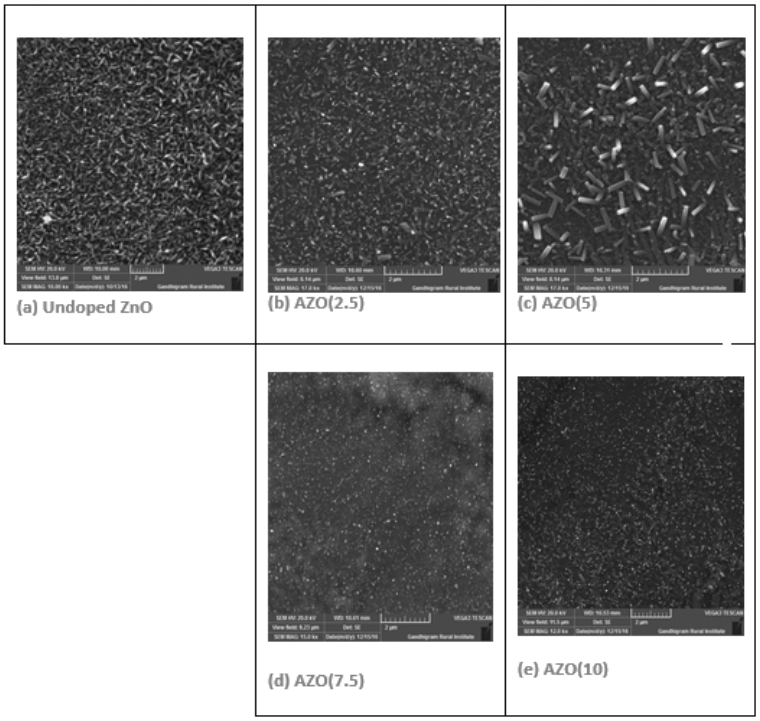

Figure 3: SEM images of ZnO thin films at different Al concentration.

The spray deposited undoped thin film exhibits spindle like nano structure, which are dense and closely packed spreading through the entire substrate surface. The doping causes significant changes in the morphology of films with different Al concentration. The AZO (2.5) film depicts the random growth of tiny nano rods on the substrate. On further increasing the Al concentration to 5% AZO(5), more prononuced nanorodscould be seen. T.Dedova et.al in their study discussed about a novel deposition method to grow ZnO nano rods by spray pyrolysis onto a ITO substrate prepared from aqueous Zinc chloride solution from the seed layer [30]. These nano rods are formed in our indigenous experimental set up, without any surfactants and seed layer For higher Al concentration the films are smooth with very small spots which can be distinguished as polycrystals.

3.2. Optical Investigations

3.2.1. UV Absorption

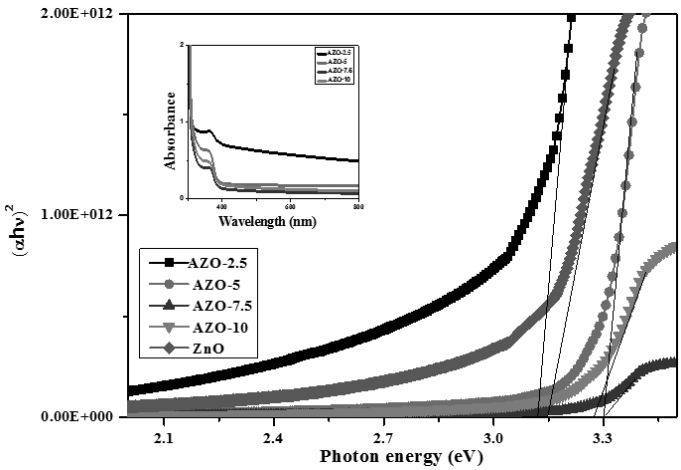

Figure 4: Optical band gap along with absorption spectra (inset) for as deposited and Al doped ZnO thin films.

The band gap (E_g) which is an important optical parameter, calculated from the absorption coefficient á which is calculated from the absorbance data. The variations of the squared absorption coefficient á, with photon energy (hí) , obey the Tauc's relation [1]

$$\alpha h\nu = A\,(h\nu - E_g)^{1/2} \qquad \textbf{(4)}$$

for direct allowed transition. This variation of (áhí) ^{2} with energy of photon (hí) was plotted and it is shown in Figure 4. The extrapolation of the linear portion of the curves to á = 0, renders the optical band gap energies. Table 3 lists the optical band gap energies (E_g) were found to vary between 3.21eV to 3.30eV. The value of band gap is 3.21eV for pure ZnO and it decreases to 3.15eV for Al doped ZnO (2.5). C. Rameshkumar et.al, found a shrinkage in optical band gap when Al at wt % is 2 [5]. The band gap value increases beyond 5 at% of AZO.

The absorption spectra (inset) shown in Figure 4 are blue shifted from 381nm to 378nm.. Yalnli Lu et.al reviewed that the blue shift in heavily doped semiconductors observed because lower energy states in the conduction band are blocked [9]. The band gap of AZO (2.5) decreases initially with the increase of doping after that band gap becomes wider. The shift in optical band gap happens due to two contending effects: band filling effect called Burstein-Moss (B-M) shift and band gap narrowing (BGN) effect. Largely BGN effect is counteracted by B-M effect because of which it is difficult to separate the two effects. So it may be attributed that due to BGN effect the band gap narrows down for AZO(2.5) sample and thereafter B-M effect dominates, causing widening of band gap for AZO(5),AZO(7.5) and AZO(10). According to Burstein-Moss

effect the band gap would increase with growing carrier concentration ($\ddot{A}E_g^{BM} \propto (3\eth^2 n_e)^{2/3}$ where n_e is the carrier concentration). Doping of ZnO with Al will expand the carrier concentration as a result, the bottom most state in the conduction band is blocked. The widening of band gap is due to the increase of Fermi level in the conduction band of the degenerate semiconductors [7].

3.2.2. Refractive index and Extinction coefficient

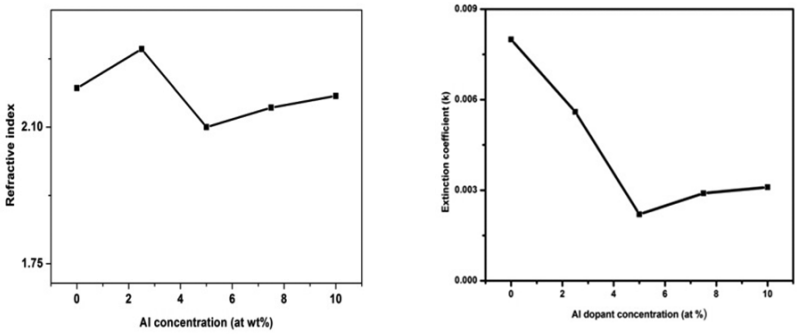

Figure 5(a) **Figure 5(b)**

Figure 5: The variation of Extinction coefficient and Refractive index with Al dopant concentration

As far as design and fabrication of optoelectronic devices are concerned, the knowledge of optical constants of materials is especially required. Index of refraction n(λ):,Extinction co-efficient k(α) , absorption co-efficient (á) are determined from the a UV-Vis absorption and transmittance spectrum. The following equations are used to calculate n(λ) and k(λ):

$$n(\lambda) = \frac{1+\sqrt{R}}{1-\sqrt{R}} \quad (5)$$

$$k(\lambda) = \frac{\alpha\lambda}{4\pi} \quad (6)$$

Where R is the reflectance, á, ë are the absorption co-efficient and wavelength. The effect of Al doping on the refractive index and extinction co-efficient are depicted in Figure 5 (a) and Figure 5(b).According to Daniel et.al the high value of n (in our case 2.30) for Al doped ZnO(2.5) thin film could be credited to an expansion in surface roughness which tends to diminish the mean free path through expanded surface scattering and makes the transparency of the films be lessened (Transparency of 60% obtained for AZO(2.5)). The lowest refractive index (n =2.11) for AZO (5) is because to grain size enhancement which results from lower strain in the deposited film. This is consistent with the estimated value of the crystallite size (Table 1).The extinction co-efficient (k) was found to fall from 0.008 to 0.0031 after doping .9 shown in Figure 5(b).

3.2.3. UV- Transmittance

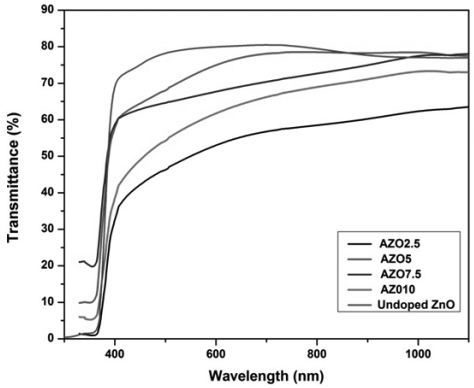

Figure 6: The optical transmission spectra of AZO thin films deposited for different Al concentrations.

Figure 6 shows the optical transmission spectra of AZO thin films coated for different Al concentrations. The transparency of the undoped films is observed to be more prominent than that of the doped films. A blue shift in the optical band edge was detected in the absorption spectra. This may be because of the presence of Al_2O_3 and Zn-O-Al phases in the synthesized films . Degradation of crystallinity causes the decrease in the transmittance of the AZO films [5].The pure ZnO and Al doped films are observed to be transparent in the visible region (400-900nm) and also in the near IR region which is a suitable factor for optical device design.

According to Burstein-Moss theory, inclusion of Al atoms shifts the Fermi level into the conduction band of semiconductors leading to the widening of band gap. Hence larger band gap would increase the optical transmission in the visible region. AZO(5) sample was recorded to have the highest transmittance of 82% and all the other films have transmittance above 70%. For doping percentages beyond 5% the transmittance decreases, this might be because of the increased phonon scattering which results in band gap widening.[1]

3.2.4. Photoluminescence Analysis.

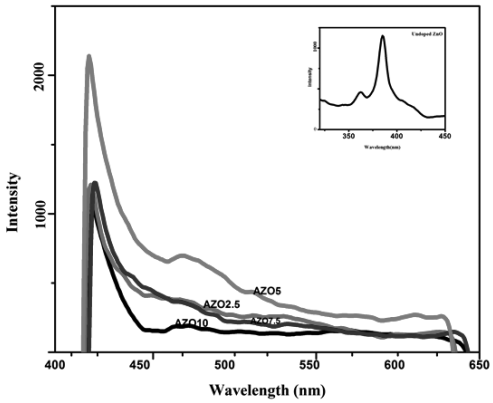

Figure 7: Photoluminescence (PL) spectra for all the four AZO thin films

Photoluminescence (PL) spectra for all the four AZO thin films are shown in Figure (7). The films are excited by Hg arc lamp at 313nm and show strong visible emission band centered around 420 nm and a hump around 494nm for all the AZO samples. The near band edge (NBE) emission centered around 380nm for pure ZnO shifts to 420nm due to Al doping .The NBE emission is due to free-exciton annihilation [31]. The maximum PL intensity was obtained for the AZO (5) sample. This may originate from the recombination of photoelectrical holes with electrons located at the ionized oxygen vacancies [11].

The blue emission in the emission spectra at 420nm (2.95eV) is inversely proportional to FTIR intensity of vibrational band at 458cm^{-1}, which is consistent with the result of PL characterization. The characteristic blue-green emission at 503nm is present at 495nm for the Al doped samples. This emission might be due to phonon-assisted transition [31,32].E.G. Bylander et.al gave a model that the blue-green emission is a result of electronic transition from an interstitial Zn to Zn vacancy [33]. The intensity of blue-green emission for the Al doped samples is decreased due to the drop in oxygen antisites and naturally the resistivity (ñ) of these films are found to be less due to this.

3.3. Electrical properties

3.3.1. Voltage-Ampere characteristics

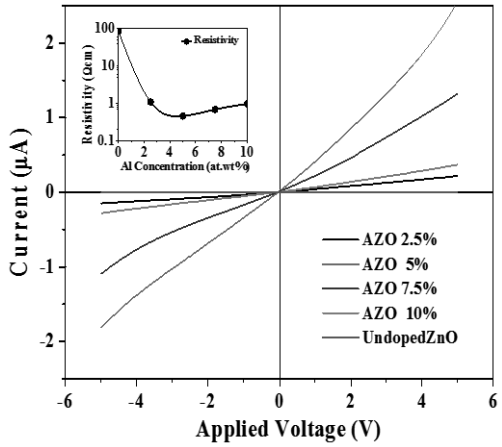

Figure 8: I-V Characteristics of AZO thin films for Al dopant concentration.

The Voltage-Current characteristics of undoped and AZO thin films were recorded by Keithley source meter. The measurements were made for voltage ranging from -5 to +5V. Figure 8 shows the variation of current (I) with voltage (V). Volatge-current characteristics of both doped and undoped Al films which are found to follow ohmic conduction mechanism . The variation of resistivity (ñ) of thin films with the concentration of Al is shown as inset in the Figure 8. The resistivity of the undoped ZnO thin films is 84 &! cm and it is reduced by two orders of magnitude to 0.45&! cm AZO (5) thin film. A. El Manouni et al got a similar result, when the Al doping concentration varied from 0 to

4%, the resistivity decreases from 45&! cm to 0.8&! cm for ZnO:Al thin films for the same substrate temperature prepared from Zinc chloride.[6]. It is inferred that the resistivity (ñ) decreases up to 5at%, implying the replacement of Zn^{2+} by Al^{3+} ions contributing more charge carriers for electrical conduction. Increase in resistivity thereafter possibly due to disorder produced in the ZnO lattice which causes the scattering of carriers such as ionized impurities and phonons [7].

3.3.2. Determination of Mobility and Carrier concentration through Hall Measurement

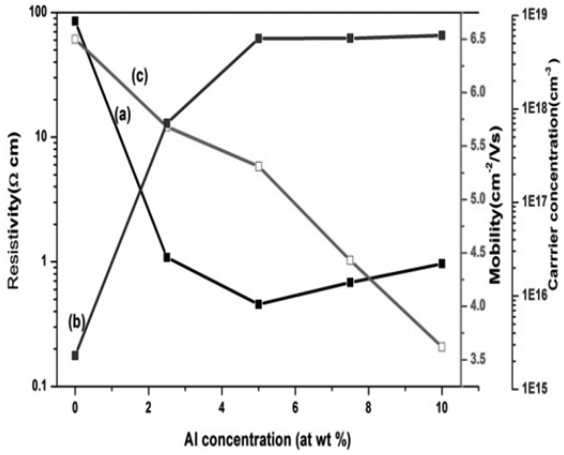

Figure 9: Variation of (a)Resistivity, (b) Carrier concentration, and (c) Mobility with Al dopant concentration

It was found that the charge carrier concentration (n_e) of AZO films increased with doping. The variation of electron concentration, mobility and resistivity with Al concentration is shown in Figure (9). The concentration of charge carriers (n_e) of 5.9 $x10^{18}$ cm^{-3} and a mobility of (μ) of $5cm^2/Vs$ was obtained for 5at% AZO films. The improvement of carrier concentration results from extrinsic donor, which is due to aluminum substitution at the Zinc site and/or the aluminum interstitials in the ZnO lattice .Thereafter the mobility of the films fond to decrease with increase in Al concentration. The earlier reports predict that, excess Al doping forms Al_2O_3, non-conducting clusters resulting in crystal disorder and defects which behave as carrier traps instead of electron donors [34, 35].This causes defects thereby inhibiting mobility of carriers at higher doping percentage.

4. Conclusion

Transparent, conductive Al doped Zinc oxide thin films are synthesized by a indigenously developed spray unit. The effect of electrical and optical properties on Al content was studied. The XRD results exhibit that all the thin films are polycrystalline with a hexagonal wurtzite structure. The films surface shows change in morphology from a spindle like nano structure to nano rods with doping. The UV-absorption studies reveal that the

absorption edges are blue shifted and the energy band gap increases from 3.21 to 3.30eV from undoped to doped samples. The pure ZnO and Al doped films are found to be transparent in the visible region (400-900nm) and also in the near IR region with a average transmittance of 82%. Optical parameters refractive index and extinction coefficient (k) are found to decrease with Al doping .Among the doped films, the AZO(5) thin film possess the best optoelectronic properties, with lowest resistivity 0.45&! cm, the carrier concentration (n_e) of $5.9X10^{18}$ cm^{-3} and a mobility of (μ) of $5cm^2/V$ sec . The experimental results show the suitability of Al doped ZnO films as transparent electrode in solar cell fabrication.

References

[1] C.M. Muiva,T.S. Sathiaraj, K.Maabong , Ceramics international **37** (2011) 555-560.

[2] M.A.Kaid, A.Ashour, Applied surface sciience **253** (2007) 3029-3033.

[3] S.Tewari, A.Bhattacharjee, Pramana-journal of physics, vol **76** (2011) 153-163.

[4] Ramakrishnan Jayakrishnan, Open Access Library Journal, **2**:e2108, http://dx.doi.org/10.4236/oalib:1102108.

[5] C.Rameshkumar, R.Subalakhmi, Journal of Chemical and Pharmaceutical Research, (2015), **7(**1):459-466

[6] A.EL Manouni,F.J. Manjon,M.Mollar,B.Mari,R.Gomez,M.C.Lopez,J.R.Ramos-Barrado, Superlattices and Microstructures **39** (2006) 185-192

[7] Rina Pandey,Shavnat Yuldashev, Hai Dong Nguyen,Hee Chang Jeon, Tae Won Kang, Current Applied Physics **12** (2012) 556-558

[8] Mujdat Caglar, Saliha Ilican, Yasemin Caglar, Fahrettin Yakuphanoglu, J Mater Sci: Mater Electron (2008) **19**:704-708

[9] Yanli Liu,Yufang Li and Haibo Zeng, Hindawi Publishing Corporation, Journal of Nanomaterials, volume 2013,Article ID **196521**, 9 pages. http://dx.doi.org/10.1155/2013/196521

[10] Khalid Dakhsi, Bouchaib Hartiti, Samira Elfarrass, HerveTchognia, Mohamed Ebn Touhami and Philippe Thevenin, MOL CRYST.LIQ.CRYST, 2016,Vol **627**, 133-140. http://dx.doi.org/10.1080/15421406.2015.1137134

[11] A.Djelloul, M-S.Aida,J.Bougdira, Journal of Luminescence **130** (2010) 2113-2117

[12] Tamiko Ohshmia,Takashi Maeda,Yuki Tanaka, Hiroharu Kawasaki,Yoshihito Yagyu,Takeshi Ihara and Yoshiaki suda, Japanese Journal of Applied Physics **55**, 01AA08 (2016) http://doi.org/10.7567/JJAP.55.01AA08

[13] M.J. Alam and D.C. Cameron, Journal of Vacuum Science and technology A 19, **1642** (2001)

[14] Z. Ben Ayadi, H. Mahdi, K.Djessas, J.L. Gauffier, L El Mir, S.Alaya, Thin Solid Films **553** (2014) 123-126

[15] Jin-Hyun SHIN, Dong-Kyun SHIN, Hee Young Lee,Transactions of nonferrous metal society of china - March 2011

[16] Y.Natsume, H.Sakata, Zinc solid films prepared by Sol-Gel Spin-Coating, Thin solid Films **372** (2000) 30-36

[17] C.R.Gorla,N.W.Emanetoglu,S.Liang,W,E.Mayo,Y.Lu,M.Wraback,H.Shen, J.Applied Physics **85** (1999) 2595-2602.

[18] J.H.Choi, H.Tabata, T.Kawai, J.Cryst.Growth **226** (2001) 493-500

[19] D.M.Bagnall, Y,F.Chen, Z,Zhu, T.Yao, S,Koyama, M.YShen, T.Goto, Applied Physics letter **70** (1997) 2230-2232.

[20] B.J.Lokhande, M.D.Uplane, Applied surface Science **167**(2000) 243-246.

[21] K.Ellmer, J.Phys. D: Appl.Phys. **33** (2000) R17

[22] Mugwangá FK, Karimi PK, Njoroge WK and Omayio O, J.Fundam Renewable Energy Appl 2015,5-4

[23] F.Paraguay, D.W,Estrada, L.D.R Acosta,N.C.Andrade, M.Miki-Yoshida, Thin Solid Films **350** (1999) 192-202.

[24] M. Chen, Z.L.Pei, C.Sun, L.S.Wen.X.Wang, Mater.Lett.**48** (2001) 194-198.

[25] D.R.Zhang, T.L.Yang,Q.P.Wang,D.J.Zhang, Mater.Chemm.Phys.**68** (2001) 233.

[26] P.Nunes, A. Malik, B.Fernandes, E.Fortunato,P.Vilarinho,R.Martis, Vacuum **52** (1999) 45.

[27] K.L Chopra, S.Major, D.K Pandyas, Thin solid films 1 (1983) 102.

[28] B.E Warren, X-ray diffraction, Dover Publications, New York (1990) p.253

[29] B.D Cullity, S.R. Stock, Elements of X-ray diffraction Third ed., Prentice-Hall, New Jersy 2001, p.170.

[30] T.Dedova, M.Krunks, M.Grossberg, O.Volobujeva, I.OjaAcik, Superlattices and Microstructures **42** (2007) 444-450

[31] P.Zu,Z.K.Tang,G.K.L Wong, M. Kawasaki, A. Ohtomo,H.Koinuma andY.Segawa, Solid stat. Commun.**103** (1997) 459-463.

[32] S.Cho,J.Ma,Y.Sun,G.K.L.Wong and J.b.Ketterson, Appl.Phys.Lett.**75** (1999) 2761-2763.

[33] E.G. Bylander, J.Appl.Phys.**49** (1978) 1188.

[34] J.Hu, R.G. Gordon, J. Appl. Phys**. 71** (1992) 880.

[35] A.F.Aktaruzzaman, G.L.Sharma, L.K.Malhotra, Thin Solid Films **198** (1991) 67.

[36] T.O.Daniel, M.Alpha and L.S.Taura, ,IOSR Journal of Applied Physics, e-ISSN: 2278-4861.Volume **7**, Issue 3 Ver.IV(May-Jun 2015),PP 20-28.